

contain H<sub>2</sub>O physisorbed on grain surfaces or interlayer surfaces in smectites (see Figs. 1b and 2a). Other materials that retain a large amount of water, as seen by a strong 3- $\mu$ m band under dry conditions (e.g., at temperatures above  $\sim 150^\circ\text{C}$ , or pressures below  $\sim 1$  mm Hg) contain H<sub>2</sub>O that is bound in the structure (see Figs. 1a, 2b, and ferrihydrite spectrum [3]). In the ferric-sulfate-doped montmorillonites water forms strong bonds to the sulfate ions because of its highly polarizing nature [7].

The hydration feature near 1.9  $\mu$ m is a combination of the H<sub>2</sub>O vibrations at  $\sim 3$   $\mu$ m and  $\sim 6$   $\mu$ m, and is also affected by the environmental conditions and the type of H<sub>2</sub>O bonding. The band strength and energy of this feature in spectra of smectites is dependent as well on the interlayer chemistry [3]. An important application to Mars is that a ferric montmorillonite in a dry environment would have a relatively weak 1.9- $\mu$ m feature that is difficult to observe in Mars spectra.

In conclusion, we would like to stress the importance of considering environmental conditions when measuring infrared spectra of laboratory samples as analogs for Mars surface materials. The strength and character of features due to molecular water ( $\sim 1.4$ ,  $\sim 1.9$ ,  $\sim 3$ , and  $\sim 6$   $\mu$ m) in the spectra of clays, palagonites, and hydrated minerals are especially sensitive to the moisture environment of the samples. These features are influenced by the exposure history (atmospheric temperature, pressure, and composition) of the samples, as well as the environmental conditions at the time of measurement.

**Acknowledgments:** The authors would like to thank Dr. A. Basilevsky for contributing the palagonites used in this study. Support through the NASA Graduate Student Researchers Program and NASA grant NAGW-28 is much appreciated. RELAB is a multi-user facility supported by NASA under grant NAGW-748, and the Nicolet was acquired by a grant from the Keck Foundation.

**References:** [1] Bruckenthal (1987) M.S. thesis, Univ. of Hawaii. [2] Bishop et al. (1993) *LPS XXIV*, 115–116. [3] Bishop et al. (1993) *GCA*, in press. [4] Bell and Crisp (1993) *Icarus*, in press. [5] Murchie et al. (1993) *Icarus*, in press. [6] Bibring et al. (1989) *Nature*, 341, 591–592. [7] Bishop et al., this volume.

56-91 ABS. ONLY  
P. 3  
N94-33196

**FERRIC SULFATE MONTMORILLONITES AS MARS SOIL ANALOGS.** J. L. Bishop<sup>1</sup>, C. M. Pieters<sup>1</sup>, and R. G. Burns<sup>2</sup>, <sup>1</sup>Brown University, Providence RI 02912, USA, <sup>2</sup>Massachusetts Institute of Technology, Cambridge MA 02139, USA.

Spectroscopic analyses have shown that Fe<sup>3+</sup>-doped smectites prepared in the laboratory exhibit important similarities to the soils on Mars [1,2]. Ferrihydrite in these smectites has features in the visible to near-infrared region that resemble the energies and band-strengths of features in reflectance spectra observed for several bright regions on Mars [3]. Ferric-sulfate-montmorillonite samples have been prepared more recently because they are a good compositional match with the surface material on Mars as measured by Viking [4]. Reflectance spectra of montmorillonite doped with ferric sulfate in the interlayer regions include a strong 3- $\mu$ m band that persists under dry conditions [5,6]. This is in contrast to spectra of similarly prepared ferric-doped montmorillonites, which exhibit a relatively weaker 3- $\mu$ m band under comparable dry environmental conditions. Presented here are reflectance spectra of a suite of ferric-sulfate-exchanged montmorillonites prepared with variable ferric sulfate concentrations and variable pH conditions.

**Experimental Procedures:** The Na and Ca interlayer cations in SWy-1 montmorillonite (Clay Mineral Society, Source Clays Repository) were exchanged with 0.5 N ferric sulfate solution in the clay suspension at pH 1.6–1.8 after titration with dilute HCl. The pH was raised dropwise with dilute NaOH to at least 3.0 in order to retain the ferric sulfate in the montmorillonite interlayer regions. The suspensions were then centrifuged and lyophilized to form a fine powder, which was dry sieved to  $<45$   $\mu$ m.

Biconical reflectance spectra were measured relative to a rough gold surface using a Nicolet 740 FTIR in a H<sub>2</sub>O- and CO<sub>2</sub>-purged environment. A PbSe detector was used from 0.9 to 3.2  $\mu$ m and a DTGS detector from 1.8 to 25  $\mu$ m. Bulk powdered samples are measured horizontally in this system. Spectra are averaged from two locations on each of two replicates for each kind of sample.

Additional bidirectional spectra were measured relative to Halon from 0.3 to 3.6  $\mu$ m using an InSb detector under ambient conditions with the RELAB (reflectance experiment laboratory) spectrometer at Brown University. A detailed description of this instrument is provided elsewhere [7].

**Results:** Reflectance spectra (0.3  $\mu$ m–3.5  $\mu$ m) of natural and chemically altered SWy montmorillonite and ferrihydrite measured under dry (H<sub>2</sub>O- and CO<sub>2</sub>-purged) conditions are shown in Fig. 1.

The spectra of each of these ferric-bearing materials exhibits absorptions in the visible region near 0.5  $\mu$ m and 0.9  $\mu$ m, an inflection near 0.6  $\mu$ m, and a reflectance maxima near 0.74  $\mu$ m, although physical and chemical constraints on the Fe<sup>3+</sup> sites in each mineral structure influence the exact energy of the crystal field transitions. The strengths of these electronic transitions are stronger in the ferric-sulfate-exchanged montmorillonites than in the other ferric-bearing materials shown in Fig. 1.

The spectra of each of these samples contain an absorption near 2.75  $\mu$ m due to OH bound to cations in the structure, and an absorption near 3.0  $\mu$ m due to H<sub>2</sub>O bound to Fe<sup>3+</sup> in the interlayer regions, H<sub>2</sub>O bound to sulfate anions, or H<sub>2</sub>O adsorbed on the grain surfaces. The ferric-sulfate-containing samples exhibit a much stronger absorption near 3  $\mu$ m and a much stronger 1.96- $\mu$ m shoulder than both the ferrihydrite and the ferrihydrite-montmorillonite.

Reflectance spectra are shown in Fig. 2 (0.3  $\mu$ m–1.1  $\mu$ m) for telescopic spectra of Mars [8], ferrihydrite-montmorillonite, and ferric sulfate-montmorillonite. This ferric sulfate-montmorillonite spectrum is that with the weakest 0.9- $\mu$ m and 3- $\mu$ m absorptions from Fig. 1. The spectra are scaled at 0.75  $\mu$ m to facilitate comparison of the spectral features.

Room-temperature Mössbauer spectra of the ferrihydrite-montmorillonite and ferric sulfate-montmorillonite are very similar; a doublet is observed with quadrupole splitting less than 1 mm/s. However, the Mössbauer spectra measured at 4.2 K exhibit a field strength of  $\sim 46$  T for the ferric sulfate-montmorillonite and a field strength of  $\sim 48$  T for the ferrihydrite-montmorillonite. The differences in field strengths of these two samples are sufficient to distinguish among them. The ferric sulfate species in the ferric sulfate-montmorillonite is also distinct from jarosite, which has a field strength of  $\sim 49$  T. Asymmetry in the peaks of the sextet in the low-temperature Mössbauer spectra of the ferric sulfate-montmorillonite may indicate that multiple ferric phases are present.

**Discussion:** The intensity of the 0.9- $\mu$ m absorption increased with ferric sulfate concentration as expected, but tends to be stronger in general than the 0.9- $\mu$ m absorption in the ferrihydrite-montmorillonite. The band center for the ferric sulfate-montmorillonite occurs

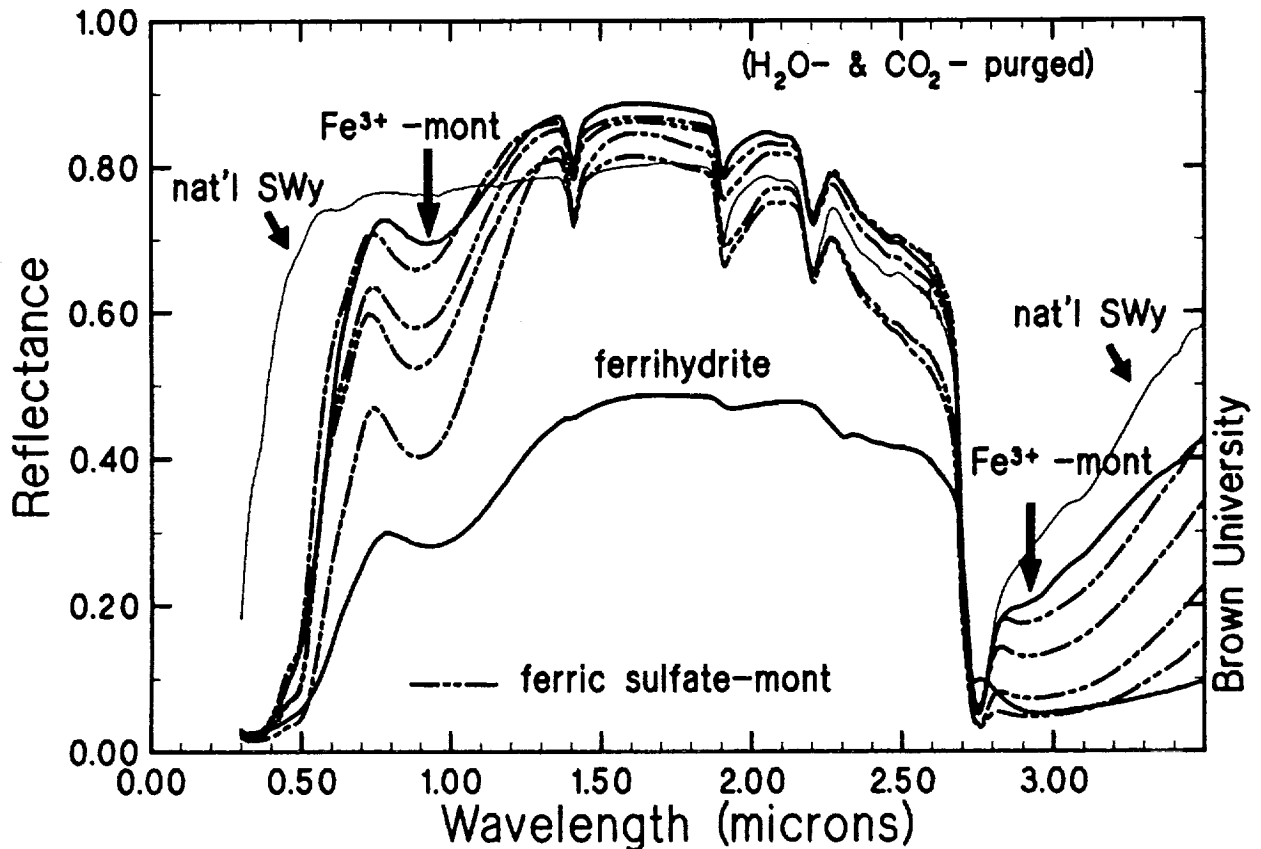


Fig. 1. Reflectance spectra (0.3–3.5  $\mu\text{m}$ ) are shown in solid lines for natural SWy montmorillonite, ferric-doped montmorillonite and ferrihydrite. Preparation of these samples is described in [2]. Spectra of four ferric-sulfate-doped montmorillonites are shown in broken lines. Increasing intensity of the spectral absorptions at 0.9  $\mu\text{m}$  and 3  $\mu\text{m}$  is observed with increasing concentration of ferric sulfate in the montmorillonite interlayer regions.

at 0.88–0.89  $\mu\text{m}$ , regardless of concentration or pH, which is a slightly shorter wavelength than that observed for the ferrihydrite-montmorillonite. The reflectance maxima varied from 0.725  $\mu\text{m}$  for the ferric sulfate-montmorillonites prepared under pH  $\sim$  3.0 to 0.745  $\mu\text{m}$  for the ferric sulfate-montmorillonites prepared under pH  $\sim$  4.0. Telescopic spectra of many regions on Mars exhibit similar visible spectral characteristics: a shoulder near 0.6  $\mu\text{m}$ , a reflectance

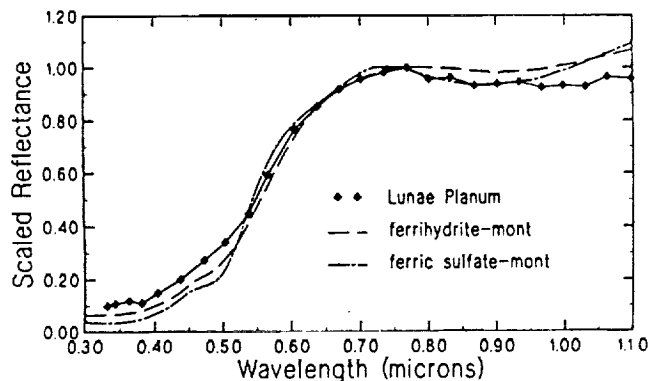


Fig. 2. Reflectance spectra of Mars and Mars analogs.

maxima near 0.74  $\mu\text{m}$ , and an absorption band near 0.9  $\mu\text{m}$  [3,8].

The intensity of the 1.96- $\mu\text{m}$  and  $\sim$ 3- $\mu\text{m}$  features in the ferric sulfate-montmorillonite spectra increased with increasing ferric sulfate concentration and increasing pH. The ferric sulfate-montmorillonite spectrum with the strongest 3- $\mu\text{m}$  absorption in Fig. 1 was also examined under extremely dry conditions; these spectra retain a strong 3- $\mu\text{m}$  band [6]. The  $\text{SO}_4^{2-}$  is highly polarizing and binds rather tightly to the interlayer water molecules in the montmorillonite. The magnitude of the  $\text{H}_2\text{O}$  absorptions may also be enhanced due to strong polarization of the  $\text{H}_2\text{O}$  molecules by the sulfate anions.

**Conclusions:** Montmorillonites doped with ferric sulfate compare well with the surface material on Mars with respect to the chemical composition and reflectance spectra in the visible to infrared. These analogs are especially promising because of the shape of the visible features and the strength of the 3- $\mu\text{m}$  band.

**Acknowledgments:** Support through the NASA Graduate Student Researchers Program and NASA grants NAGW-28 and NAGW-2220 is much appreciated. RELAB is a multi-user facility supported by NASA under grant NAGW-748, and the Nicolet was acquired by a grant from the Keck Foundation.

**References:** [1] Banin and Rishpon (1979) *J. Molec. Evol.*, 14, 133–152. [2] Bishop et al. (1993) *GCA*, in press. [3] Bell et al. (1990) *JGR*, 95, 14447–14461. [4] Clark et al. (1982) *JGR*, 87,

10059-10067. [5] Bishop et al. (1993) *LPS XXIV*, 115-116. [6] Bishop et al., this volume. [7] Mustard and Pieters (1989) *JGR*, 92, 10376-10390. [8] McCord et al (1977) *Icarus*, 31, 25-39.

57-91 ADS ONLY

N94-33197

**CONSTRAINTS ON THE MARTIAN CRATERING RATE IMPOSED BY THE SNC METEORITES AND VALLIS MARINERIS LAYERED DEPOSITS.** J. E. Brandenburg, Research Support Instruments, Alexandria VA, USA.

**Introduction: Martian Cratering Rate and Mars Past:**

The rate at which craters form on the martian surface is a crucial parameter for understanding the geologic history of that planet. However, until samples can be returned from known locations on Mars, the rate of cratering cannot be correlated accurately with geologic ages but must be estimated. In this paper an attempt is made to use two separate bodies of data that seem incongruous with currently accepted models for correlating cumulative crater densities with geologic ages: the measured depths of the interior layered deposits in the Candor Chasma region [1] and nearby areas of the Vallis Marineris system and the measured cosmic ray exposure times and crystallization ages of the SNC meteorites [2], to constrain estimates of the martian cratering rates. That is, rather than considering these two bodies of data to represent special or peculiar circumstances in conventional cratering age schemes, we instead assume they represent conventional circumstances and attempt to find what adjustments to present cratering-age correlation models are required for the models to be reconciled. The preliminary results of this study indicate that the interior layered deposits, which may be lake sediments dating from the "liquid water era" on Mars (the period when large amounts of liquid water apparently helped shape the planets surface), and the SNC meteorites, which are believed to represent samples of the martian surface carried to Earth by one or several impacts on the martian surface, independently constrain the past martian cratering rate to be many times the past lunar cratering rate.

Several models for correlating geologic ages with cumulative crater densities have been proposed [3,4]. These models assume that the rate of crater formation has varied in time beginning with an intense period of bombardment shortly after the formation of the planet followed by a period of lower cratering rate in the later periods of planetary history. The models differ principally in their assumed rate of cratering in this later period. These rates are usually represented as being a multiple of the lunar rate of cratering, the Moon being the one planetary surface where cratering history has been preserved and from which samples have been returned. The models of Neukum and Hiller [5] are most illustrative of this type of model and demonstrate that if the rates of martian cratering are assumed to be 1, 2, and 3x the lunar rate (Neukum and Hiller models I, II, and III respectively, hereafter referred to as NHI, NHII, and NHIII) then the picture of Mars varies dramatically. The difference between the history of Mars under NHI and NHIII is the difference between a planet whose climate was Moon-like and one that was Earth-like for much of its history (see Fig. 1).

Under NHI the cratering rate is assumed to be lunar, and the erosive rate must be low to give the observed cumulative crater densities. What results is a very lunar set of ages for many martian surface formations, and an age for most water channels that is very old, indicating that Mars must have had a dense Earth-like atmos-

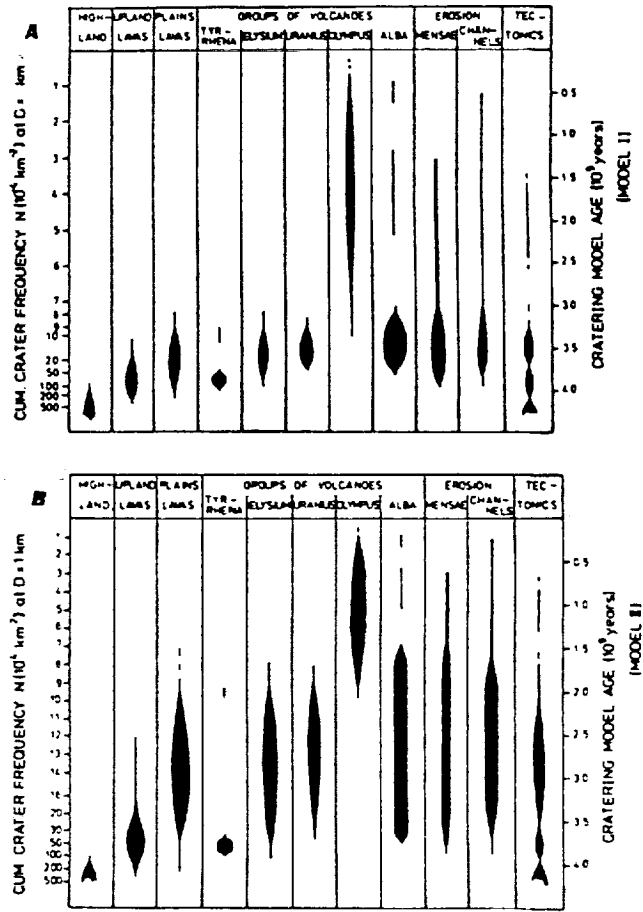


Fig. 1. (a) Neukum-Hiller model I: Mars cratering rate same as for the Moon. (b) Neukum-Hiller model II: Impact fluxes factor of 2 higher than on the Moon.

phere and temperatures for only a geologically brief period of 1 b.y. This means that most liquid-water-produced features must have ages of 3.5 b.y. and mean surface ages of approximately 3.0 b.y. However, under NHII Mars was a dynamic changing planet for most of its history, with the liquid water era and vigorous channel formation lasting until late in the planet's history. The effect of the 2x lunar cratering rate assumed under NHII is not only to make the mean age of large areas of the martian surface younger but also to increase the variation of ages. This occurs because (1) the ages of many surface formations that were formerly confined to a narrow range of ages between 3 b.y. and 4.5 b.y. are now expanded across the span of martian history, and (2) the model is consistent with an Earth-like climate for Mars for much of its history, allowing free movement of liquid water across its surface. The model NHII is thus consistent with water-formed features late in the planet's history and a mean surface age of approximately 2 b.y. The consistency of NHII and the even more extended model NHIII with late water-formed features allows features such as the Candor Chasma layered sediments to be accommodated easily without recourse to special models.

**Layered Deposits of Candor and Associated Chasmas of Vallis Marineris:** The interior layered deposits seen extensively